NDT&E International 158 (2026) 103555

Contents lists available at ScienceDirect

NDT and E International

journal homepage: www.elsevier.com/locate/ndteint

Quantitative phase characterisation of nickel-based superalloy Inconel 718 using ultrasound

Jennifer H. Jobling [a,d,*], Edward A. Saunders [b], Stacy Moore [c], Mark C. Hardy [d], Tim Barden [b], Michael J.S. Lowe [a], Bo Lan [a,**]

[a] Department of Mechanical Engineering, Imperial College London, SW7 2AZ, UK
[b] Rolls-Royce plc., Bristol, BS34 7QE, UK
[c] School of Physics, University of Bristol, BS8 1TL, UK
[d] Rolls-Royce plc., Derby, DE24 8ED, UK

A B S T R A C T

Phase composition in nickel-based superalloy Inconel 718 is a determinant factor of its overall mechanical properties. Ultrasound has been shown to have sensitivity to the phases through its wave speeds in a previous qualitative feasibility study. This paper demonstrates the capability of ultrasonic wave speed (UWS) measurements for the quantitative characterisation of delta (δ) phase in the nickel-based superalloy Inconel 718, which is fundamentally due to the zeroth spherical harmonic coefficient of velocity, V00, being sensitive to changes in microstructure. A variety of samples having undergone different processing histories were used for the UWS measurements, alongside extensive metallurgical investigations – including advanced microscopy techniques such as high-speed atomic force microscopy (HS-AFM), as well as hardness testing to fully understand the microstructures of each sample and corroborate the UWS results. By combining the data from these experimental techniques, and through an iterative parameter search, it was confirmed that the V00 measurements could be used to deduce the δ phase content in the Inconel 718 samples; more significantly, the strength of a combined materials characterisation framework – incorporating UWS measurements, hardness testing and microscopy – was demonstrated, establishing a powerful tool for the phase characterisation of nickel-based superalloys for the future.

1. Introduction

The nickel-based superalloys are a group of materials of huge importance across the engineering industry, due to their superior mechanical properties at elevated operating temperatures and ability to withstand extremely harsh conditions. The extensive use of these nickel-based superalloys across various applications in aerospace [1–6], nuclear [7,8] and chemical industries [9], often in critical components, requires a robust and reliable method for the monitoring and characterisation of their microstructure throughout their lifecycle to ensure that they are still meeting requirements. Indeed, microstructural evolution in time during service (such as variation in phase composition, or the precipitates present) which may arise from unpredictable stresses, strains, and thermal conditions due to anomalous operating conditions, could impact material properties, and subsequently both the component's short- and long-term performance [10].

As discussed by Jobling et al. [10], the main existing microstructural characterisation methods available are, in general, destructive, requiring metallurgical sectioning with long overall preparation and inspection times. In addition to optical microscopy, these include scanning electron microscopy (SEM), electron backscatter diffraction (EBSD), and transmission electron microscopy (TEM), which do offer extremely high spatial resolution but with very stringent sample size limitations, particularly for EBSD [11] and TEM [12]. Although the process of surface polishing and etching itself can be used to assess local microstructure in a component, it is not entirely non-destructive and limited to local areas; indeed, the polishing can affect part dimensional tolerances, and etching can reduce component fatigue life. The more recent technique of Spatially Resolved Acoustic Spectroscopy, or SRAS [13,14] is theoretically non-destructive, and has been developed for deployment on rough surfaces [15]; however, current inspections require polishing to a very smooth finish, and thus the total time of inspection is still relatively long. In addition, SRAS does not have sufficient resolution to detect changes in phase composition of very small-scale precipitates. All of these techniques have the further disadvantage of being surface inspection techniques only. The most powerful bulk characterisation techniques of neutron diffraction [16,17] and X-ray synchrotron [18–20] measurements also have their limitations in terms

* Corresponding author. Department of Mechanical Engineering, Imperial College London, SW7 2AZ, UK
** Corresponding author. Department of Mechanical Engineering, Imperial College London, SW7 2AZ, UK.
E-mail addresses: j.jobling18@ic.ac.uk, jennifer.jobling2@rolls-royce.com (J.H. Jobling), bo.lan@imperial.ac.uk (B. Lan).

https://doi.org/10.1016/j.ndteint.2025.103555
Received 18 June 2025; Received in revised form 19 September 2025; Accepted 19 September 2025
Available online 24 September 2025
0963-8695/© 2025 The Authors. Published by Elsevier Ltd. This is an open access article under the CC BY license (http://creativecommons.org/licenses/by/4.0/).

of sample size, and the high energies required – in addition to the challenge of acquiring access to the limited number of facilities available. There is therefore still the need for a non-destructive, robust, inexpensive, and easily accessible method for the bulk characterisation of material microstructures for the nickel-based superalloys, as microstructural characteristics – including phase composition – are highly influential on material performance.

It was successfully demonstrated in a feasibility study [10] that there was the potential for ultrasonic wave speed (UWS) measurements to detect microstructural variation in nickel-based superalloy Inconel 718. This study built on previous work by Lan et al. [21,22], which had established that the wave speeds in a polycrystal can be expressed as a convolution between material texture and single crystal wave speeds, using a spherical harmonic expansion framework. The zeroth order expansion coefficient of the polycrystal in this convolution, V00, corresponds to the average wave speed across all 3D propagation directions, and it was demonstrated in the study that phase changes (resulting from heat treatments) resulted in small but consistent and unquestionably measurable changes in V00. This conclusion, as well as the fact that V00 is also independent of texture, rendered the UWS technique a promising method in the characterisation of phase composition of materials [23]. The underlying theoretical framework is also independent of frequency, meaning that the inspections can be scaled as necessary for component dimensions or material grain size.

As discussed, this feasibility study presented an exciting opportunity for the non-destructive testing (NDT) of engineering materials, establishing a foundation for the development of a reliable, non-destructive materials characterisation technique with rapid feedback which could quickly analyse materials and components to ensure they were still suitable for use in service. Indeed, one particular benefit of this method is its ability to offer a statistical average measurement through the material volume in the thickness direction, rather than solely surface (or sub-surface) information, and thus negating the need for multiple layer inspections. If these UWS measurements were also incorporated into a broader materials characterisation methodology which included other established metallurgical techniques, such as hardness testing and microscopy, this would further enhance the strength of this ultrasonic inspection method – creating a holistic and robust materials characterisation framework that would give a detailed insight into the microstructure of a material or component, enabling further understanding of its behaviour. This is what the work discussed in this paper, drawing on material from the author's doctoral thesis, is aiming to accomplish.

Having completed the feasibility study and successfully demonstrated the V00 measurement's sensitivity to phase changes within Inconel 718, the further work in this paper has focussed on the quantitative estimation of phase composition within this nickel-based superalloy; for these investigations, the delta (δ) phase has been selected as an example. Additional experimental methods have also been incorporated into this work, including hardness testing and high-speed atomic force microscopy (HS-AFM) imaging, in order to fully understand the microstructures of the samples being used, and begin laying the foundations for a larger characterisation framework. Indeed, the detailed metallurgical examinations undertaken, as well as extensive ultrasonic wave speed measurements for each sample, have provided a deeper understanding of the expected microstructures, and the corresponding mechanical and ultrasonic behaviours, which have undergone a variety of different processing histories.

This paper will first summarise the experimental materials used for this study and the rationale behind selecting the specific heat treatment processes used, before detailing the results; first, from the UWS measurements, where the data from 16 rounds of experiments showed a clearly observable and quantifiable convergence to different V00 values for each of the sample microstructures, as well as from the metallurgical investigations which included hardness measurements, optical microscopy and SEM, and HS-AFM. Having gained a detailed insight into the microstructures, the phase estimation investigations could then be carried out, of which the key trials and iterations have been included. In addition, the strength of a combined characterisation framework, incorporating UWS measurements, has also been demonstrated through the discovery that the samples in their as-received condition did not have a suitable microstructure for use in-service. The paper concludes with a brief discussion of these results and analyses, and outlines future work to further refine the technique for phase composition estimates in other materials within the nickel-based superalloy family.

2. Materials and Methodology

The following section outlines the experimental materials and processing used for these studies, as well as the various metallurgical techniques used to analyse the microstructural characteristics of each sample to compare with the UWS measurements. A flowchart of the techniques in the order of use for these investigations is shown in Fig. 1 to summarise the experimental work for this study. These techniques include SEM, for the initial verification that the heat treatments had impacted the microstructures of the samples as required (in the elimination/formation of the δ phase), followed by HS-AFM, for higher resolution imaging of the microstructures, and topographical analysis of the surface, to validate the findings from SEM inspections. The Vickers hardness testing was performed in order to link the hardness values of particular microstructures to V00 measurements, and begin the compiling of a dataset which could be used for a holistic characterisation framework. It should be noted that the microscopy was carried out to investigate the microstructures prior to the UWS measurements for this study, but when deploying this characterisation framework in industry, the experiments would be led primarily by the UWS measurements. For a full description of the underlying theoretical framework and experimental procedure for UWS measurements, as well as a discussion on the microstructure of Inconel 718, the reader is referred to earlier publications by the authors [10,23].

2.1. Experimental materials

For these investigations, five samples were machined from a billet of Inconel 718, heat treated to AMS 5662 (comprising a solution treatment between 941 and 1010 °C followed by an air cool), purchased from a commercial supplier. These were each ~5 mm thick with a diameter of approximately 70 mm, for which a sample holder in a dodecagon shape was designed to enable accurate rotations for the UWS measurements. The heat treatment processing then followed, having selected the δ phase to investigate quantitative phase characterisation for Inconel 718. This selection was primarily due to its relative ease of manipulation, compared to the other major precipitate phases such as the gamma prime (γ') and gamma double prime (γ'') – from the classic time-temperature-transformation (TTT) diagram of Inconel 718 proposed by Oradei-Basile [24], shown in Fig. 2, it can be seen that there are no regions where solely the γ' or γ'' can be isolated. Additional challenges of using these precipitates include their extremely small scales, which can be difficult to detect visually, even with high resolution microscopy. Conversely, it can be seen that there is a large region where there should, in theory, be solely the δ present, and there is also the fact that this phase naturally forms as much larger particles within Inconel 718, enabling much easier detection. Although the δ precipitate does not contribute directly to the strengthening of the material, it is key in the grain size control [9] as well as improving stress rupture ductility [1] and is therefore still an important phase to be able to quantify.

The TTT diagram for Inconel 718 was used to develop the appropriate heat treatments for the experimental samples. The aim was to generate two contrasting microstructures with regards to δ phase content; first, a microstructure with the maximum amount of δ phase possible, and another which was nominally precipitate-free. One of the five discs was retained in the as-received condition, supplied as

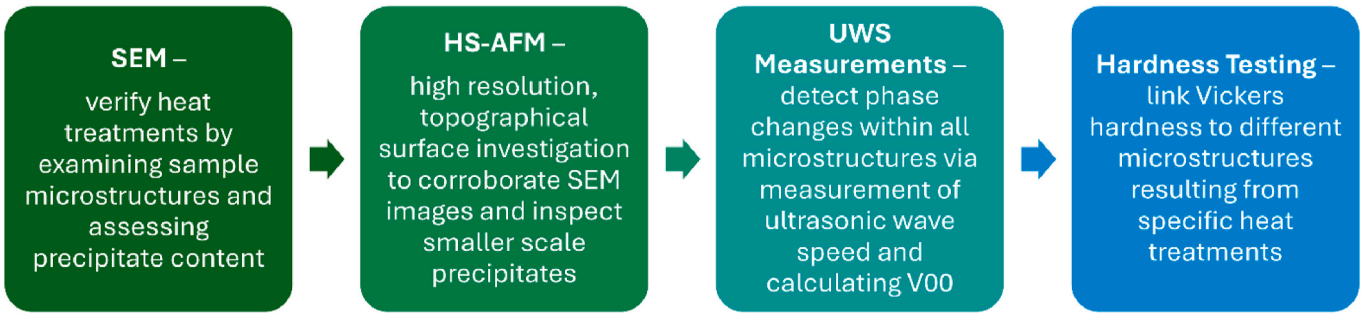


Fig. 1. Schematic to summarise experimental techniques.

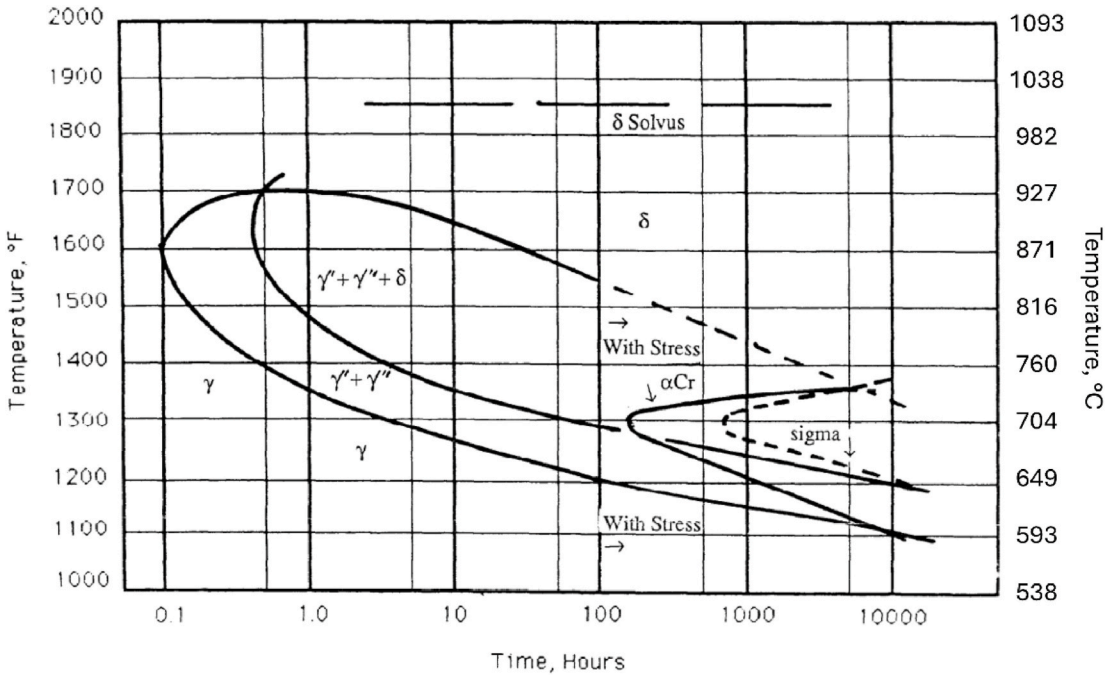


Fig. 2. Time-Temperature-Transformation (TTT) diagram adapted from Oradei-Basile [24], depicting expected phase content in Inconel 718 under various thermal and temporal conditions.

conforming to AMS 5662 (referred to as the 'Datum' sample); one disc was then subjected to a heat treatment of a hold at 900 °C for 50 h followed by a water quench ('WQ900'), and another held at 1000 °C for 10 h followed by a water quench ('WQ1000'). The two remaining discs were also subjected to these heat treatment procedures, but erroneously furnace cooled, allowing all of the precipitates to come out of solution. However, these were retained and also used for experiments to investigate the applicability of the V00 measurements, denoted 'FC900' and 'FC1000', where 'FC' represented furnace cooling, followed by the temperature of holding. For the phase quantification studies, additional discs of Inconel 718 (previously used for the feasibility study) were also utilised; these were denoted OG1HD, OG2HD, OG3 and OG4, where 'OG' denotes original (in the as received, AMS 5662 solution treated condition) and 'HD' a heat damaged sample, where the heat treatment simulating 'heat damage' involved a hold at 1100 °C for 4 h, followed by an oil quench. Detailed microstructural analysis of these samples can be found in a previous publication [10].

It has been assumed for this study that the acoustoelastic effects of residual stress are negligible, as per prior work by Lan et al. [21–23]. The machining of the samples has a release effect of the macro- and intergranular residual stresses, with predominantly intragranular residual stresses remaining; the additional heat treatments for the majority of the samples result in a further reduction, due to an annealing effect. The impact of these residual stresses on the ultrasonic wave speeds is expected to be small, and is planned to be investigated further in future studies.

2.2. *Metallurgical investigations*

To corroborate the findings of the UWS measurements, a number of different metallurgical techniques were utilised to gain a detailed understanding of each of the sample conditions being examined for this study. In addition to conventional methods, including optical microscopy, SEM and hardness testing, there was also the opportunity to use the more advanced technique of high-speed atomic force microscopy, or HS-AFM. This latter technique offers the ability to topographically image microstructures at extremely high resolution (of up to 1–2 nm lateral resolution, dependent on tip radius, compared to the 10 nm achievable by SEM [25]) by traversing a very fine cantilever tip, of less than 10 nm radius [26], across a sample surface; in addition to the greater resolution achievable compared to SEM, the fact that it is a topographical imaging method means that it is possible to eliminate uncertainties which can arise in SEM micrograph analysis, such as whether a surface feature is due to a precipitate being present or some remaining residue from the preparation process. (In this instance, the method was employed to further study and understand the distribution

and presence of γ'/γ'', which was precluded by the SEM investigation.) Although there are several different configurations available, the setup used for these investigations involves a laser Doppler vibrometer (LDV) detection system measuring the cantilever tip displacement, with the HS-AFM in contact mode. The UWS measurements, for which the metallurgical investigations were used to corroborate, are described in the following section.

2.3. UWS measurements and phase estimations

The UWS measurements were carried out using the experimental setup described in previous publications [10,23], with 16 individual trials carried out for each sample; each consisted of 3 individual runs of the experiment, with an average V00 value taken after each trial. The measurements are obtained with using an immersion tank setup, comprising a non-focussed 10 MHz transducer in pulse-echo configuration, of 6 mm diameter and 69 mm near-field length. The sample is supported between the transducer and an acoustic mirror at the base, in order to allow for the through-transmission ultrasonic signals to be acquired. Once the calibration procedure is complete (which involves scanning the sample from end to end to ensure that there is zero sample tilt, to within ± 3 μm tolerance, and that the transducer is perpendicular to the sample surface), the tilting of the sample during data acquisition is fully automated. A full statistical analysis of the error associated with this approach can be found in the prior feasibility study [10]. Having acquired the V00 values, the following equation could be used to estimate the amount of δ phase present within a given sample in terms of its volume fraction h, assuming it is solely the γ matrix and δ precipitates present [10]:

$$V_{00}|_{overall} = V_{00}|_{\delta}(h) + V_{00}|_{\gamma}(1-h) \quad (1)$$

When using the single crystal elastic constants (SCECs) for the individual phases, however, it is the single crystal coefficient, K_{00}, which is calculated; this is simply related to the zeroth order velocity coefficient, V_{00}, via the following, which can instead be used in Equation (1) –

$$K_{00} = V_{00}\sqrt{4\pi} \quad (2)$$

Although this phase quantification technique is therefore reliant on knowledge of SCECs of the individual phases of interest within the material – which may be more challenging to acquire, particularly for smaller scale precipitates – experimental data from V00 measurements can be used to approximate these values in the first instance, and verified against metallurgical examinations of materials. The results and data obtained from all experiments are discussed in the following section.

3. Results and Analyses

This section will first detail the findings of the microscopy investigations across the samples, before moving on to the UWS measurements; further investigation of the materials, using hardness measurements, have then been included, as well as a brief discussion of the consolidated results across the techniques. Having acquired the V00 measurements, the phase quantification trials could begin, the results of which have been summarised to conclude the section.

3.1. SEM examinations

To ensure that the heat treatment processes had resulted in the intended microstructures for the study, small 5 mm-sided cubes were machined off the edge of each disc, and prepared for microscopy using the polishing and etching process detailed previously [10]. Figs. 3–6 show the SEM images obtained across the samples; the low magnification images of Datum and WQ1000 (Fig. 3a and b) appear to be as expected, with the needle-like δ phase visible on the grain boundaries for the former, and absent from the latter due to the fast cooling preventing the precipitate from re-forming. Higher magnification micrographs are shown of FC900, FC1000, and WQ900 in Fig. 4; it can be seen that the 900 °C heat treatment has been extremely effective in precipitating the δ phase, as it is not solely forming on the grain boundaries but also within the grains themselves. The more typical precipitation behaviour of the δ phase can be seen in the microstructure of FC1000, where the slow cooling rate has allowed this precipitate to reform (largely at grain boundaries).

Further higher magnification images of FC900 and WQ900 are shown in Figs. 5 and 6, with the background mottling visible in Fig. 5b tentatively proposed to be the γ'/γ''. Although the presence of these precipitates in FC900 was predicted, the fact that the mottling in the WQ900 sample (which suggests they may also be present here) was more unexpected, as this heat treatment was determined with the aim of isolating the δ phase without the formation of other precipitates. To confirm that these were precipitates, rather than surface residues or etch-pitting features, the WQ900 sample was also examined using the topographical microscopy technique of HS-AFM.

3.2. HS-AFM micrographs

Some HS-AFM images acquired of WQ900 are shown in Fig. 7. Fig. 7a shows a composite image of several consecutive tiles acquired using the HS-AFM, stitched together and then analysed using the Gwyddion [27] software, with Fig. 7b an individual image from a scan of the WQ900

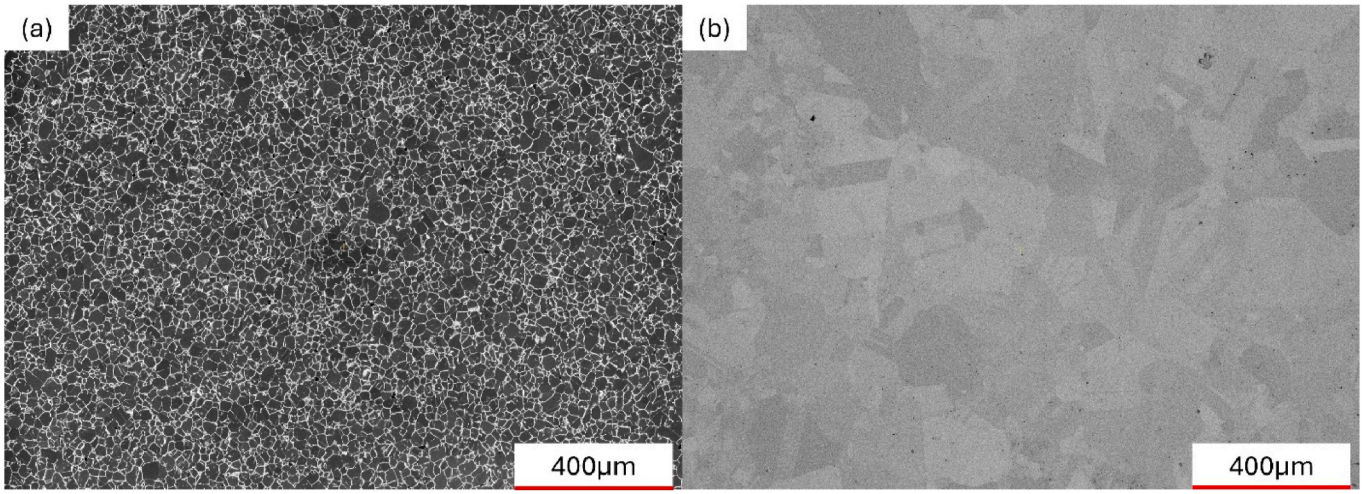


Fig. 3. Low magnification SEM images of (a) Datum and (b) WQ1000.

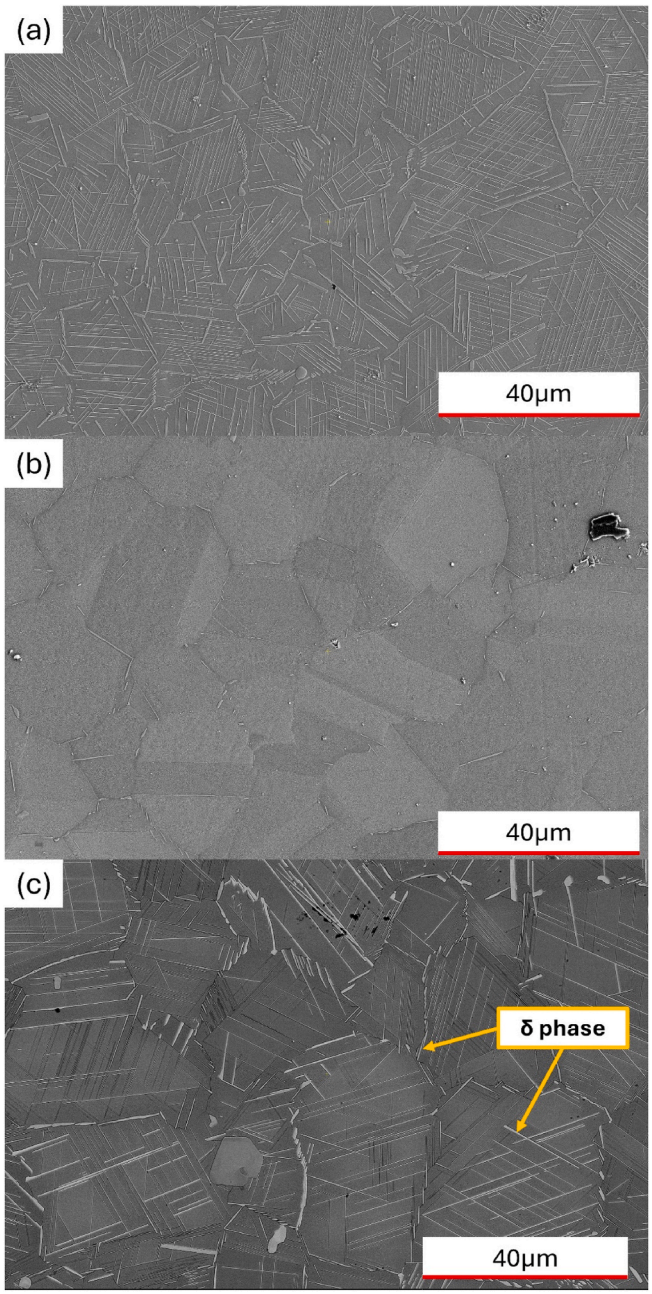


Fig. 4. SEM images of (a) FC900, (b) FC1000, and (c) WQ900. The high levels of δ phase precipitation is visible in FC900 and WQ900, with sparse needles only on the grain boundaries in FC1000.

sample surface. The fact that the background mottling seen in the SEM images is now clearly visible as precipitate in the HS-AFM micrographs creates surety that, despite the high temperature hold and rapid cooling, the γ'/γ'' have not been eliminated completely from the microstructure of the sample as intended. This may be due to the fact that the water quenching rate was not sufficiently fast to suppress the γ'/γ'' from returning out of the solution, due to the volume of water being too small to rapidly cool the material fully down to room temperature. The fact that these precipitates are present in the WQ900 sample implies that they are present across all of the Inconel 718 samples used. Although the volume fraction, size and morphology of these γ'/γ'' will differ, and may account for some variability in the V00 measurements, it is known that there is a significant volume fraction of γ'/γ'' present across all the samples; it has therefore been assumed for the purposes of this study that that the effect of the γ'/γ'' on V00 is constant, and hence the overriding effect of the larger δ phase can be studied and explored for the phase estimation trials.

The following section will discuss the UWS measurements acquired in order to begin the quantitative estimation of the δ precipitate within the Inconel 718 samples.

3.3. Ultrasonic wave speed measurements

The cumulative mean V00 from the ultrasonic experiments are shown in Fig. 8, from which it can be seen that, not only is there a clear convergence to an average V00 for each sample condition, but that the average V00 is reached after approximately 8 experiments. As well as illustrating the convergence towards a 'true' mean V00, the cumulative averaging process is used to reduce the errors in these measurements. A detailed statistical analysis of this experimental technique can be found in previous publications [10,28]. However, the interpretation of these results was not as straightforward as initially theorised; it had been assumed that the greater the proportion of a stiffening and strengthening precipitate, such as the δ phase, the higher the overall wave speeds which would result in a higher V00 value. The values shown in Fig. 8, however, do not align with this trend; the Datum sample, which should have more of the δ phase present than WQ1000, exhibits the lowest V00, with the WQ900 also being unexpectedly low in the overall ranking of V00. One possible explanation proposed was that the excessive precipitation of the δ phase, with a saturating effect on the microstructure effect on the microstructure inside the grains, may have had a retarding effect on the wave speeds, though this was deemed unlikely given that the V00 is theoretically only affected by chemical and compositional changes. Before proceeding with the phase estimates, however, the final metallurgical technique planned for this study – Vickers hardness measurements – was carried out for each of the samples, to investigate whether there may be any other factors affecting the wave speed results.

3.4. Vickers Hardness testing

In order to acquire Vickers hardness data for the samples, a standard Vickers mechanical hardness tester with a 30 kg load was used (both UCAS accredited) and calibrated with a control sample of nickel prior to testing of the samples. Three indentations were made in each sample in the ground, polished, and etched condition; the average of the diagonal lengths was used to calculate the HV30 value for each sample, which have been plotted against the zeroth coefficient of velocity, V00, in Fig. 9. The indentations were made at least 3 diagonal lengths apart, to ensure that they did not interfere with the other indentation results; as each indentation had a length of around 500 μm, it was assumed that the hardness measurement would be a good representation of the bulk material (with the largest δ precipitates being no more than 40 μm in length). For completeness, two Inconel 718 samples used in the previous feasibility study [10] – OG, representing a sample in the as-received condition, and OGHD, a heat-damaged sample – have been included here. Although the two measurements are quantifying slightly different phenomena (with a hardness test indicating resistance to plastic deformation, whereas ultrasonic velocity is most significantly impacted by elastic stiffness), the hardness does relate to the elastic modulus, and a positive correlation is expected. The UWS measurements are predominantly affected by changes of phase (with density also having an effect, but to a lesser extent) – similar to the main factors influencing material hardness, in addition to the microstructure and grain size. As shown in Fig. 9, there was indeed a strong positive correlation between the HV30 and V00 of each sample, with a Pearson correlation coefficient r of 0.83.

Despite this correlation, however, there are some noticeable outliers of this trend – these are the water quenched samples, WQ900 and WQ1000. It is proposed that these samples' deviation from the overall line of best fit could be rationalised by the effects of solid solution strengthening, or lack thereof – which may also explain the order of the V00 values for the samples. The V00 of WQ900 sitting below the line of

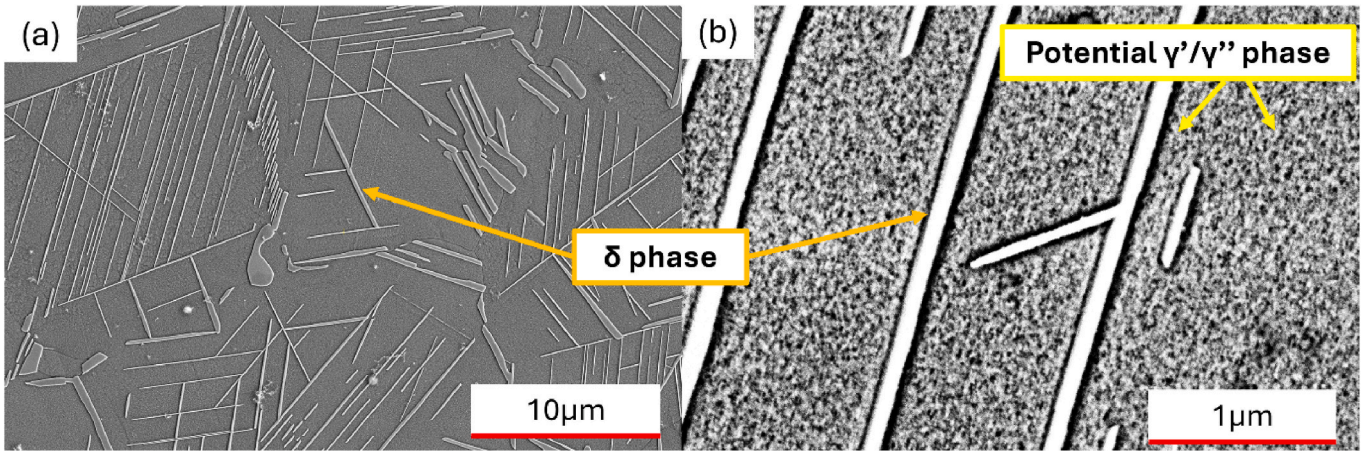


Fig. 5. SEM Micrographs of FC900, with the needle-like δ phase clearly identifiable. It is thought that the background mottling in (b) may be the γ'/γ'' precipitates, but cannot be resolved for certain in the SEM.

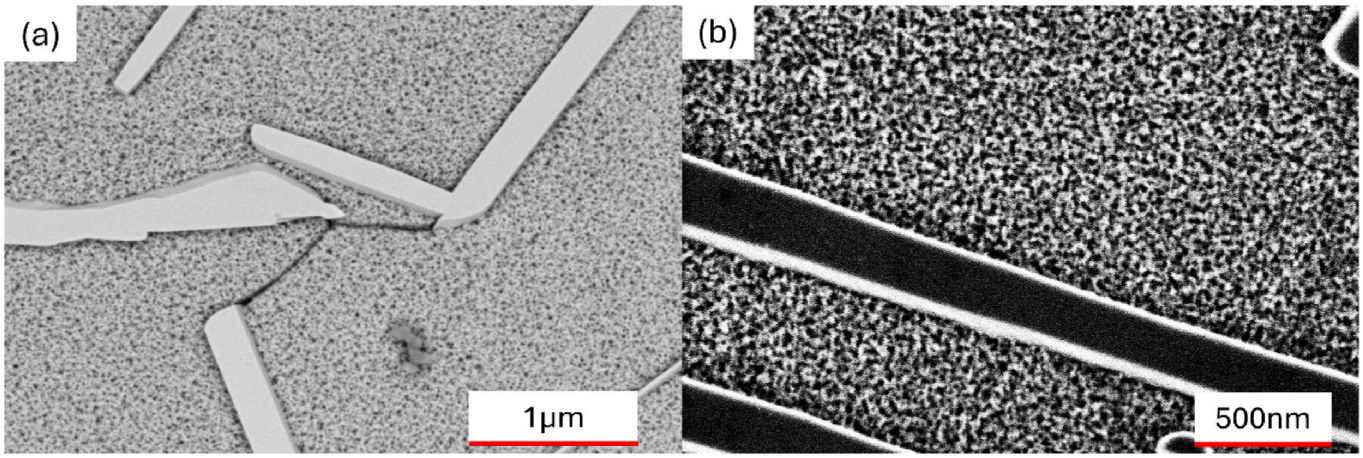


Fig. 6. Higher magnification SEM micrographs of WQ900; the background mottling appears to be comparable to the tentatively identified γ'/γ'' observed in the FC900 sample, despite the intention of the 900 °C heat treatment of eliminating all but the δ phase.

best fit may be due to a lack of solid solution strengthening, where the excessive precipitation of the δ phase may have resulted in a deficit of some of the elements (namely Nb, with the δ phase having the composition Ni_3Nb) which may have otherwise provided the matrix with elastic stiffness. Conversely, the result of WQ1000 could be due to an opposite effect, where elements from other precipitates which have been taken back into solution (such as molybdenum, titanium and niobium [29,30], all of which are present in the γ'' phase [31]) may in turn have returned to the matrix and provide a solid solution effect – contributing to an overall more elastically stiff structure, but with no change in the resistance to plastic deformation. The effects of solid solution strengthening being responsible for the outlying results would be an interesting investigation to pursue using more in-depth microscopy examinations in the future; further HS-AFM imaging would also be useful in a more detailed study of the γ′ and γ'' present.

In addition to providing insight into the impact of solid solution strengthening on the V00 measurements, and an explanation as to why the V00 measurements of the samples were not in the expected order, a further key finding from these tests was the extremely low hardness of the Datum sample compared to the typical value of Inconel 718, which should have a HV30 value of around 400 [32]. The fact that the Datum sample had the lowest V00 of all the samples, combined with the low hardness, posed the question of whether this sample did indeed have the expected microstructure of Inconel 718 in a service deployable condition; if this were the case, the strengthening precipitates (γ′ and γ'', as well as the δ phase) should be present to an extent where the V00 value would be larger than the WQ1000 sample. These combined results led to further investigation of the sample billet specification, where it was subsequently found that – although the material had been supplied to conform to AMS 5662 (the standard Inconel 718 specification) – it had been solution treated only, and not aged; it is the latter ageing stage which is key in allowing for the strengthening precipitates to be brought out of solution.

This analysis proved to be an excellent demonstration of the potential place of V00 measurements within a materials characterisation framework; the fact that the microstructure was nonconformant to the required specification was deduced from combined experimental data of V00 and HV30 measurements (which additional microscopy may also support) was an excellent example of how the V00 technique could be deployed in industry when assessing materials or components for microstructural changes. Having established that the Datum sample had not been fully aged, however, it was decided that this should be aged to be fully conformant to AMS 5662, as it would be useful for the V00 technique to be trialled on a sample relevant to industrial applications. The ageing comprised a hold of 720 °C for 8 h, followed by a furnace cool to 620 °C after which there was a further hold for 8 h, and finishing with an oil quench [33]. The heat treatment schematic is shown in Fig. 10, and was carried out on a previously investigated sample of Inconel 718 in the as-received condition, OG3; these generated new microstructures, for which the samples were named DatumA and OG3A

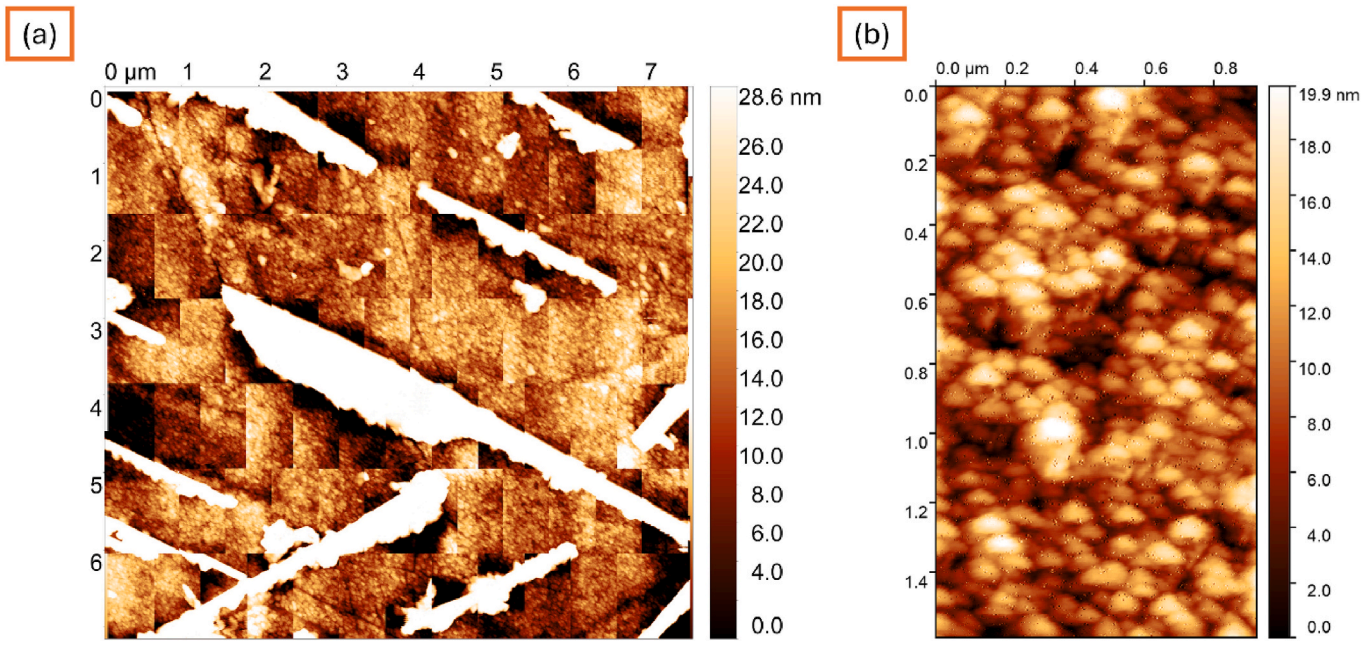


Fig. 7. HS-AFM images of the WQ900 sample, where (a) is a composite image of several individual image tiles, such as that shown in (b). The δ phase needles are the larger white particles in (a), with the γ'/γ'' clearly visible in (b). The γ'/γ'' appear triangular in some instances due to the cantilever tip becoming blunt over the course of scanning.

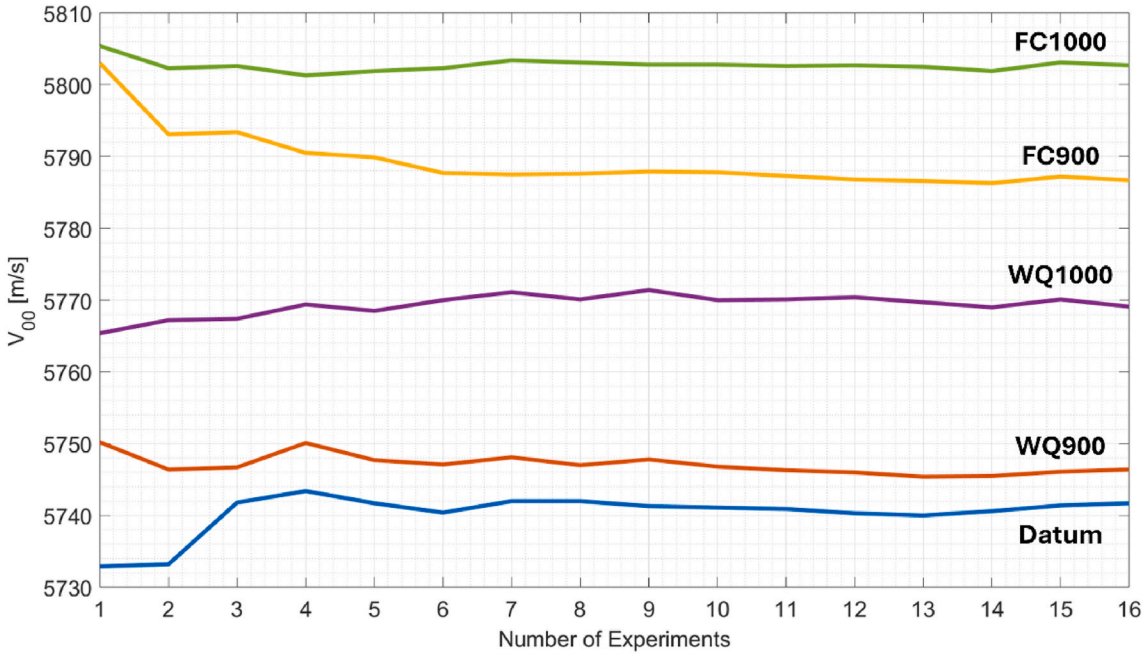


Fig. 8. UWS results showing the cumulative average V00 for each of the Inconel 718 samples.

respectively (with A denoting 'aged'). On testing in the UWS water tank, it was confirmed that the V00 measurements were significantly higher than the other sample microstructures (with just FC1000 having a higher V00 value than the DatumA sample). The cumulative mean V00 values for each of the samples are tabulated below together with the hardness values to summarise, where the V00 of the OG samples have been taken from the prior feasibility study [10]. Table 2 gives the average grain size for each of the sample heat treatments for completeness. It should be noted that the grain size was assessed using a linear intercept methodology, examining one area in a microsection for each sample; a visual assessment confirmed that the measurement was representative of the whole image. However, despite the fact that the individual measurement may not be representative of the average grain size in that particular sample, each heat treatment condition comprised multiple sample measurements, and hence the average grain size quoted is a good indication of the typical grain sizes expected for each sample condition.

On completing the UWS measurements and the metallurgical analyses to fully understand the sample microstructures, the quantitative estimation of the δ phase using the V00 results could then be studied. These trials will be discussed in the following section.

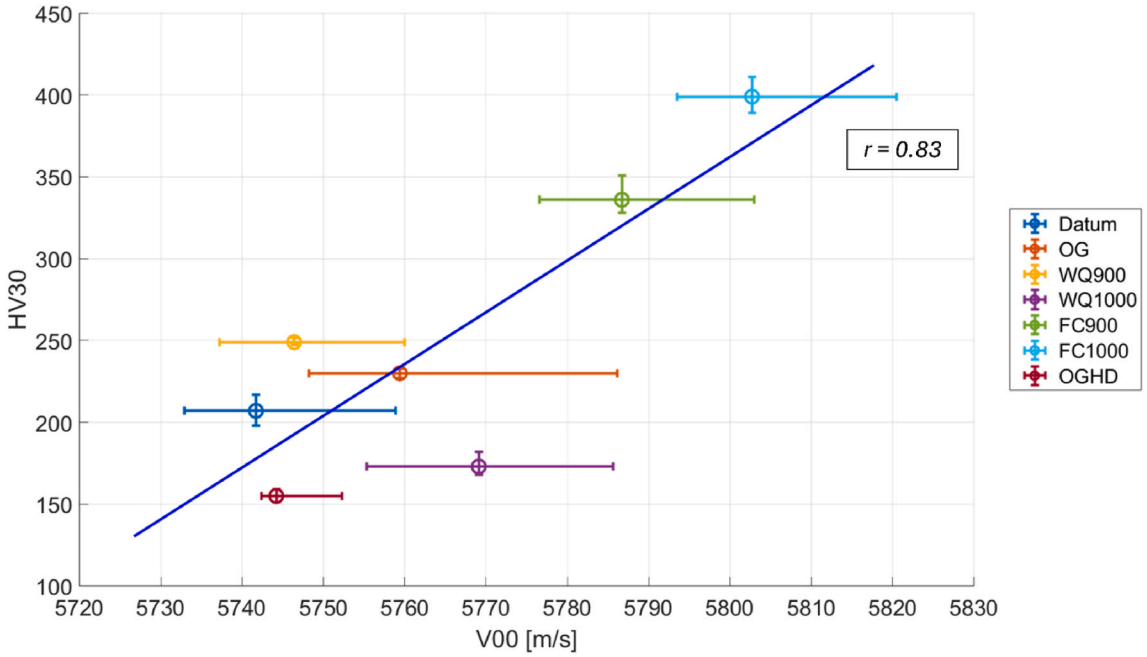


Fig. 9. Graph to show correlation between Vickers Hardness and V00 of Inconel 718 samples. There is a positive correlation between these measurements, with a Pearson correlation coefficient of 0.83.

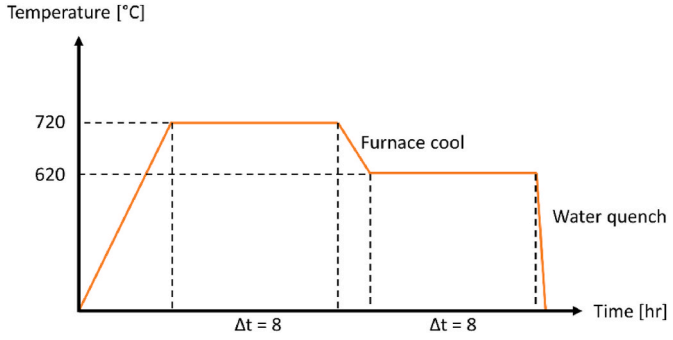


Fig. 10. Heat treatment schematic for ageing process of Inconel 718, according to specification AMS 5662.

4. Quantitative Estimation of δ Phase

The first stage in the estimation of the δ phase proportion involved finding the zeroth coefficient of the single crystal elastic constant, K00, of both the γ matrix as well as the δ phase, in order to deploy the phase estimation equation derived in previous work [21–23]. The main difficulty was posed by the fact that, unlike those for the alpha and beta phases in titanium (for which the phase estimation has been successfully demonstrated [28]), the SCECs of each of the phases within Inconel 718 were not widely known. In addition, there was the additional challenge of not being able to obtain accurate percentages of the δ precipitate present from the samples themselves. It was the intention to use an accessible image analysis software to estimate the amount of δ from the micrographs obtained, but it was found that the area shading was inconsistent and highly inaccurate; any estimates acquired in this method would also have been a 2D slice from a small area only, rather than a realistic 3D representation. It was therefore necessary to use consolidated data acquired from the UWS experiments, combined with microstructural studies reporting phase percentages for given heat treatments in the literature, to first estimate suitable values for both the γ and δ phases. From the metallurgical examinations and as discussed in Section 3.2, it has been assumed that the γ′ and γ′′ precipitates are present across all samples which have not been 'heat damaged', and assumed to have a negligible effect on the phase estimates (with respect to the variations in the amount of δ present).

Table 1
Summary of Inconel 718 samples, with V00 and HV30 values.

Sample	Heat Treatment	V00 [m/s]	Hardness (HV30)
OG1HD	Hold at 1100 °C for 4 h, oil quench	5.7442 × 10^3	155
OG2HD	Hold at 1100 °C for 4 h, oil quench	5.7442 × 10^3	
OG4HD	Hold at 1100 °C for 4 h, oil quench	5.7391 × 10^3	
OG3	N/A	5.7588 × 10^3	230
OG4	N/A	5.7600 × 10^3	
OG3A	Hold at 720 °C for 8 h, furnace cool to 620 °C, hold for 8 h, water quench	5.7995 × 10^3	434
Datum	N/A	5.7417 × 10^3	207
WQ900	Hold at 900 °C for 50 h, water quench	5.7464 × 10^3	249
WQ1000	Hold at 1000 °C for 10 h, water quench	5.7691 × 10^3	173
FC900	Hold at 900 °C for 50 h, furnace cool	5.7869 × 10^3	336
FC1000	Hold at 1000 °C for 10 h, furnace cool	5.8027 × 10^3	399
DatumA	Hold at 720 °C for 8 h, furnace cool to 620 °C, hold for 8 h, water quench	5.7916 × 10^3	434

From the numerous iterations which were investigated, there were three trials – denoted A, B, and C – which resulted in estimating realistic proportions of the δ phase. All of these used the K00 of OG4HD, 20344.58 m/s (calculated from the V00 value of 5739.1 m/s as given in Table 1), to approximate that of the γ matrix; this was then used, with a K00 calculated using combinations of the aged samples' V00 values (OG3A and DatumA), to approximate the K00 of the γ phase, assuming a

Table 2
Average grain size measurements for Inconel 718 heat treatments.

Heat Treatment	Samples	Grain Size	
		ASTM Value	Average Size [micron]
None	OG3, OG4, Datum	8.95	16.67
900 °C for 50 h	WQ900, FC900	8.35	19.32
1000 °C for 10 h	WQ1000, FC1000	5.38	88.64
1100 °C for 4 h	OG1HD, OG2HD, OG4HD	0.67	248.66
720 °C for 8 h, 620 °C for 8 h	OG3A, DatumA	8.00	22.75

4.2 % δ phase composition typically found in fully aged Inconel 718 [34]. The K00 values used to represent the δ phase for each trial are shown for reference in Table 3, together with the corresponding V00 values; the results of the δ phase estimates using these values are given in Table 4, together with the average across all trials. By using experimental data, this approach had the advantage of essentially giving a 'homogenised' K00 value for the γ matrix which would include any γ′ and γ'' particles present. An additional point to note was that the K00 of the γ matrix aligned closely with that of Inconel 718 (calculated using the SCECs from Ref. [35] to then solve the Christoffel equation of anisotropic media [36]), further validating these values; there was also the fact that the K00 values of the γ and δ phase were far apart, which has been known to improve accuracy in phase estimations [28].

All of the iterations generated erroneous results for the WQ900 sample, giving δ phase proportions much lower than observed from the obtained micrographs; however, this was to be expected, as the V00 of this sample was significantly lower than the other samples (and indeed, lower than the OG samples' before heat treatment). The WQ900 sample was therefore not considered when assessing the feasibility and accuracy of the V00 phase estimation approach. It can be seen, however, that for the other samples there were still reasonable and realistic estimates of the proportion of δ phase present, including OG3 and OG4, as well as FC1000, from comparison to the literature-reported values. The differences between the estimated δ proportions across the trials are of a very small order, and the aged samples both have predicted δ phase amounts which line up well with the average of 4.2 % [34] – for DatumA, between 3.65 % and 3.91 %, and for OG3A between 4.20 % and 4.83 % (although, as variant B solely used OG3A to represent K00 for the δ phase, this yielded the exact value of 4.20 %). In addition, the percentages of δ phase in the WQ1000 sample of between 2.09 % and 2.40 % were initially thought to be inaccurate; however, it was subsequently found that this in fact aligns well with the literature reported value of having around 3 % δ phase [37] (despite this heat treatment being given specifically to eliminate all precipitates).

For the samples OG3 and OG4, the lower percentages of the δ phase predicted could be explained by their being not fully aged, and hence the precipitates were not able to form completely. The higher percentage of the δ phase in sample FC1000 could be rationalised by its being held at a higher temperature than the aged samples, potentially allowing more time for the δ phase (albeit in addition to other precipitates) to form in comparison to the OG samples; however, the predicted amount of δ phase is still realistic, and corresponds to the δ phase precipitation visible on the grain boundaries. Further analyses of the phase estimation results are presented in the following section.

Table 3
K00 values used for each trial variation, with corresponding V00 values for reference.

Variation	δ phase		
	K00 [m/s]	V00 [m/s]	Source
A	25109.90	7083.37	OG3A/DatumA
B	25443.55	7177.49	OG3A
C	24776.24	6989.25	DatumA

4.1. Analyses of phase estimation results

Despite the lack of available literature data for the SCECs of the γ and δ phases within Inconel 718, this study still generated some key results in terms of the application of V00 measurements to the quantitative estimation of the δ phase in Inconel 718; not only was it shown that there were realistic estimates of the δ phase percentage generated, but through these investigations it has been possible to identify a range of K00 values that these phases could be expected to have, to be used for future experimental work.

Across the various trials of δ phase estimation, it was found that the V00 of OG4HD to represent the γ phase was the optimal value; this was likely due to its being the lowest of all HD samples, and thus resulting in the maximum difference possible between the K00 of the γ and δ phases, as well as being unlikely to result in negative phase proportion estimates (which had previously been observed in earlier attempts). The fact that the 'HD' heat treatment temperature was above the δ solvus temperature of 1000 °C [24][38] meant it was the most likely material condition to be free of the δ phase, and hence validated its use for estimating a K00 value for the γ matrix (or, as the case may be, a homogenised value for the γ matrix which included any γ'/γ'' which may have remained, or been on the cusp of formation).

Of all variants, Trial A appears to have the best compromise across all of the samples, with the amount of δ phase in the HD samples being close to 0 %, the aged samples close to the theoretical 4.2 %, and the WQ1000 sample predicted to have a similar value to the 3 % also reported in the literature. The FC1000 sample also predicted a similar amount of the δ phase to WQ1000, which is a promising result given the same hold temperature and time.

Through carrying out these studies, some key discoveries were made which highlighted additional aspects for consideration when using the V00 technique for phase quantification; most significantly, it was observed that this phase estimation technique using UWS measurements may not be applicable for all conditions of Inconel 718 (or indeed, any nickel-based superalloy) where there is excessive precipitation of a

Table 4
Results of trials A, B, and C, and their average, for estimating the δ phase within each sample.

Variation	Estimated δ phase [%]			
	A	B	C	Average
Feasibility Study Samples				
OG1HD	0.38	0.35	0.41	0.38
OG2HD	0.38	0.35	0.41	0.38
OG4HD	0.00	0.00	0.00	0.00
OG3	1.47	1.37	1.58	1.47
OG4	1.55	1.45	1.67	1.56
OG3A	4.49	4.20	4.83	4.51
Present Study Samples				
Datum	0.19	0.18	0.21	0.19
DatumA	3.91	3.65	4.20	3.92
WQ900	0.54	0.51	0.58	0.54
WQ1000	2.23	2.09	2.40	2.24
FC900	3.56	3.32	3.82	3.57
FC1000	4.73	4.42	5.09	4.75

particular phase, such as the δ phase in WQ900, which yielded such a low measurement of V00 that any phase estimations for this sample would be highly inaccurate. One challenge which was not anticipated was the acquisition of a visual validation of these phase composition estimates; attempts to use conventional image analysis tools were unsuccessful due to inconsistencies and inaccuracies in shaded regions, and in imaging the samples using high resolution EBSD scans it was found that the sample drift was too large to obtain micrographs which could be used. Conversely, it was found that lower resolution maps had insufficient contrast to detect the δ phase. However, the micrographs of WQ900 (see Fig. 4c) were useful in justifying the elimination of this sample when considering the accuracy of the δ phase estimation, as it was immediately apparent that the low V00 was an outlier, and for its extremely high precipitate content a higher value would have been expected.

5. Discussion

Despite the challenges encountered during the phase estimations, the fact that the obtained estimates aligned well with the literature were promising, and indicated the potential of this method to be further developed and refined for accurate phase quantification. Indeed, a key outcome was the calculation of a range of K00 values, without the SCECs of the γ and δ phases being available, which could be used for future phase estimations on different samples of Inconel 718. Also highlighted through these experiments was the observation that the effect of a precipitate's morphology, and extent of formation, could have on V00 measurements; for example, the γ′ and γ'' not being fully precipitated in the heat damaged samples clearly having a lower impact on the overall wave speeds, such that they were far removed from those of the other materials which had been subjected to different processing. In the WQ900 sample, it was observed that the excessive amounts of δ phase did have a drastic effect on the ultrasonic wave speeds, but it was clear that the greater the amount of a strengthening precipitate did not necessarily correspond to a higher V00 measurement. The cause of this would be an interesting investigation to pursue in the future.

Throughout these experiments and investigations, it has become apparent that the microstructure of Inconel 718 – and its behaviour having undergone different heat processing – is far from straightforward. As this UWS phase estimation technique can only be deployed effectively for dual phase materials, it has been the case that the more complex microstructural characteristics of Inconel 718 has made the quantitative estimation of the δ phase more challenging than expected, and future work could focus on deploying this UWS phase estimation on dual-phase nickel-based superalloys, such as Udimet 720Li or RR1000. Nevertheless, it was found that the phase estimates could be successfully deployed in some instances, and there have now been generated a set of K00 values for the γ and δ phases which could be used for phase estimations in the future. An additional point to note is that these variations could be detected even when they were small (for example, between 4.2 % for the aged samples compared to 0 % δ phase in the heat damaged samples), a promising aspect of this technique which has also been demonstrated.

A further exciting outcome from these investigations is the successful deployment of the UWS measurements, in combination with other metallurgical methods, in being able to determine that a sample was not suitable for industrial use. From the extremely low V00 of the Datum sample relative to others of Inconel 718, it was possible to immediately deduce that its microstructure was not as expected, which was then corroborated by hardness tests (and higher magnification microscopy may have also been able to validate these results). This discovery was possible despite the lack of available data for a fully conformant sample of Inconel 718; the fact that there is now a full set of V00 measurements for each sample condition available means that this will be more straightforward in the future.

Indeed, the UWS measurement technique alone would have numerous advantages to both research and industrial applications; not only does it offer a high inspection efficiency, due to the speed of acquiring the UWS measurements as well as the rapid feedback of results, but is also a low cost technique. There is no sample surface preparation required, and the components required to assemble the full water tank and sample rotation system are inexpensive, as well as being very easily accessible, and can thus be adapted to suit the application and environment – whether in a research laboratory, or on a larger scale production line. With the V00 measurements giving a bulk average of the overall microstructure, there is not the need for inspections in multiple orientations, hence further increasing inspection efficiency compared to other microstructure inspection methods, such as EBSD. The nature of the frequency-independence of the spherical convolution framework offers additional advantages; samples are not limited in size, and the frequency of inspection can be adapted as required. The measurements are also not limited by the requirement for the piezoelectric transducer and water tank setup, which currently limits the samples which can be inspected to having parallel sides; other emerging techniques, including laser ultrasound excitation or resonant ultrasound spectroscopy (RUS) could instead be used, enabling a more flexible approach to inspections [10].

Incorporating these UWS measurements as part of a framework would enable an even more robust inspection technique; there could also be further developments to integrate ultrasonic attenuation measurements, which are more closely coupled with grain size, another key microstructural characteristic which affects mechanical behaviour; this could offer an additional non-destructive method to the overall framework, and provide further insight into the overall microstructure of a sample. By testing a range of different sample conditions, a database of different values for different materials could be compiled, enabling a quick comparison following an inspection – similar to comparing the diagonal of a hardness test indentation to a Vickers hardness chart. In the future, the use of ultrasonic inspections alone – the UWS measurements together with attenuation characterisation – could minimise the need for destructive inspection techniques, or those which are theoretically non-destructive but can increase risk of damage; the indentations required for hardness testing, for example, can increase the risk of crack propagation, or create fatigue initiation sites [10]. The use of hardness tests is often used to indicate changes in fatigue life during service life, which is closely linked to grain size; thus, attenuation measurements could potentially be used instead, reducing the time of inspection as well as minimising the risk of damage to the component.

6. Conclusions

Having previously demonstrated in a feasibility study that the zeroth spherical harmonic coefficient of velocity, V00, was sensitive to microstructural changes within nickel-based superalloys, this experimental technique has been investigated further and applied to samples of Inconel 718 with specific processing programmes, with the aim of eliminating all precipitates except for the δ phase within the main γ matrix, to begin phase estimation trials. Two heat treatments were developed, with the aim of precipitating the maximum amount of δ phase possible, as well as generating a nominally precipitate-free microstructure. A total of five new sample microstructures were generated; in addition to the Datum sample, the two heat treatments were carried out with both furnace cooling and water quenching after finishing the hold at temperature. These samples were used alongside 4 discs of Inconel 718 used for a previous feasibility study [10]. The experimental results and subsequent analyses can be summarised as follows –

1. The UWS measurements of these samples demonstrated a high level of consistency; the cumulative mean value of V00 was approached after 8 experiments across all samples, converging to separate, distinguishable values.

2. Subsequent metallurgical investigations, including conventional electron microscopy and hardness tests as well as the more advanced high-speed AFM, revealed that these heat treatments had not been successful in completely eliminating the γ′ and γ'' phases; however, for the purposes of this study, the γ'/γ'' proportion in each sample was considered to have a consistent effect on the V00 results, and hence a quantitative estimation of the effect of the δ phase could be made.
3. Although there was no available data in the literature for the SCECs of the γ and δ phases in Inconel 718, there were promising results from these trials of phase estimates carried out using the experimental V00 measurements, with there being realistic proportions of this phase predicted across the samples (excluding WQ900, which had an abnormally low V00 for its δ phase content), comparing favourably with the literature. Through the course of these investigations, a range of values for the single crystal elastic term, K00, of the γ and δ phases in Inconel 718 have been estimated, which could be used for additional investigations.

Finally, further analysis – in comparing these V00 measurements with Vickers hardness values of each sample – proved to be an excellent demonstration of how a materials characterisation framework, incorporating V00 measurements, could be deployed in research and industry alike. The fact that the Datum sample did not have a service-useable microstructure was rapidly deduced using a combination of these techniques, led predominantly by the abnormally low V00 value. This conclusion was despite the fact that there was little experimental data available; the fact that there have since been extensive investigations, and subsequently an increase in the expected V00 and hardness values for a given processing history, means that future deductions will be much more straightforward, thus representing an exciting application of the UWS measurement technique in the future.

CRediT authorship contribution statement

Jennifer H. Jobling: Writing – review & editing, Writing – original draft, Methodology, Investigation, Formal analysis, Data curation. **Edward A. Saunders:** Writing – review & editing, Supervision, Resources, Investigation, Formal analysis, Data curation. **Stacy Moore:** Writing – review & editing, Resources, Methodology, Data curation. **Mark C. Hardy:** Writing – review & editing, Supervision, Resources. **Tim Barden:** Supervision, Conceptualization. **Michael J.S. Lowe:** Writing – review & editing, Supervision, Conceptualization. **Bo Lan:** Writing – review & editing, Supervision, Software, Methodology, Funding acquisition, Conceptualization.

Declaration of competing interest

The authors declare that they have no known competing financial interests or personal relationships that could have appeared to influence the work reported in this paper.The authors declare the following financial interests/personal relationships which may be considered as potential competing interests:

Acknowledgements

The authors would like to thank EPSRC (EP/L015587/1) and Rolls-Royce plc for the funding for this project, Antonio de Sanctis for assistance with experimental equipment, and Dr Ming Huang for advice regarding statistical analysis (both of Imperial College London). BL wishes to acknowledge the support from the Imperial College Research Fellowship Scheme.

Data availability

Data will be made available on request.

References

[1] Reed RC. The superalloys: fundamentals and applications. Cambridge: Cambridge University Press; 2008.
[2] Amiri A, Bruschi S, Hossein Sadeghi M, Bariani P. Investigation on hot deformation behavior of waspaloy. Mater Sci Eng, A 2013;562:77–82.
[3] Utada S, Sasaki R, Reed RC, Tang YT. Overheating of waspaloy: effect of cooling rate on flow stress behavior. Mater Des 2022;221:110911.
[4] Liu F, Chen J, Dong J, Zhang M, Yao Z. The hot deformation behaviors of coarse, fine and mixed grain for udimet 720Li superalloy. Mater Sci Eng, A 2016;651:102–15.
[5] Chang L, Jin H, Sun W. Solidification behavior of Ni-base superalloy udimet 720Li. J Alloys Compd 2015;653:266–70.
[6] Jackson MP, Reed RC. Heat treatment of UDIMET 720Li: the effect of microstructure on properties. Mater Sci Eng, A 1999;259(1):85–97.
[7] Jang C, Lee J, Kim JS, Jin TE. Mechanical property variation within inconel 82/182 dissimilar metal weld between low alloy steel and 316 stainless steel. Int J Pres Ves Pip 2008;85(9):635–46.
[8] Panneerselvam G, Raju S, Jose R, Sivasubramanian K, Divakar R, Mohandas E, Antony MP. A study on the thermal expansion characteristics of Inconel-82® filler wire by high temperature X-ray diffraction. Mater Lett 2004;58(1–2):216–21.
[9] Appa Rao G, Srinivas M, Sarma DS. Influence of modified processing on structure and properties of hot isostatically pressed superalloy inconel 718. Mater Sci Eng 2006;418(1–2):282–91.
[10] Jobling JH, Saunders EA, Barden T, Lowe MJS, Lan B. A feasibility study on phase characterisation of nickel-based superalloys using ultrasound. NDT E Int 2024:103120.
[11] Charpagne M-A, Vennegues P, Billot T, Franchets J-M, Bozzolo N. Evidence of multimicrometric coherent γ′ precipitatesin a hot-forged γ–γ′ nickel-based superalloy. J Microsc 2016;263(1):106–12.
[12] Parsa AB, Ramsperger M, Kostka A, Somsen C, Korner C, Eggeler G. Transmission electron microscopy of a CMSX-4 Ni-Base superalloy produced by selective electron beam melting. Metals 2016;6(11):258.
[13] Sharples S, Clark M, Somekh MG. Spatially resolved acoustic spectroscopy for fast noncontact imaging of material microstructure. Optic Express 2006;14:10435–40.
[14] Clark M, Sharples SD, Somekh MG. Fast, all-optical rayleigh wave microscope imaging on isotropic and anisotropic materials. IEEE Trans Ultrason Ferroelectrics Freq Control 2000;47(1):65–74.
[15] Li W, Dryburgh P, Pieris D, Patel R, Clark M, Smith RJ. Imaging microstructure on optically rough surfaces using spatially resolved acoustic spectroscopy. Applied Sciences 2023;13(6):3424.
[16] Turner RP, Panwisawas C, Lu Y, Dhiman I, Basoalto HC, Brooks JW. Neutron tomography methods applied to a nickel-based superalloy additive manufacture build. Mater Lett 2018;230:109–12.
[17] Grant BMB, Francis EM, Quinta da Fonseca J, Daymond MR, Preuss M. Deformation behaviour of an advanced nickel-based superalloy studied by neutron diffraction and electron microscopy. Acta Mater 2012;60(19):6829–41.
[18] Epishin A, Camin B, Hansen L, Chyrkin A, Nolze G. Synchrotron Sub-μ X-ray tomography of kirkendall porosity in a diffusion couple of nickel-base superalloy and nickel after annealing at 1250C. Adv Eng Mater 2021;23:2001220.
[19] Link T, Zabler S, Epishin A, Haibel A, Bansal TX. Synchrotron tomography of porosity in single-crystal nickel-base superalloys. Mater Sci Eng, A 2006;425(1–2):47–54.
[20] le Graverend J-B, Jacques A, Cormier J, Ferry O, Schenk T, Mendez J. Creep of a nickel-based single-crystal superalloy during very high-temperature jumps followed by synchrotron X-ray diffraction. Acta Mater 2015;84:65–79.
[21] Lan B, Dunne FPE, Lowe MJS. A generalized spherical harmonic deconvolution to obtain texture of cubic materials from ultrasonic wave speed. J Mech Phys Solid 2015;83:221–42.
[22] Lan B, Dunne FPE, Lowe MJS. A spherical harmonic approach for the determination of HCP texture from ultrasound: a solution to the inverse problem. J Mech Phys Solid 2015;83:179–98.
[23] Lan B, Britton TB, Jun T-S, Gan W, Hofmann M, Dunne FPE, Lowe MJS. Direct volumetric measurement of crystallographic texture using acoustic waves. Acta Mater 2018;159:384–94.
[24] Oradei-Basile A, Radavich JF. A current T-T-T diagram for wrought alloy 718. In: *Superalloys 718, 625 and various derivatives*, warrendale, PA, the minerals, vol. 1991. Metals & Materials Society; 1991. p. 325–35.
[25] Payton OD, Picco L, Scott TB. High-speed atomic force microscopy for materials science. Int Mater Rev 2016;61(8):473–94.
[26] Klapetek P, Necsas D. "gwyddion," department of nanometrology. Czech Metrology Institute; 2024 [Online]. Available: http://gwyddion.net/. [Accessed 28 June 2024].
[27] Lan B, Britton TB, Jun T-S, Gan W, Hofmann M, Dunne FPE, Lowe MJS. Direct volumetric measurement of crystallographic texture using acoustic waves. Acta Mater 2018;159:384–94.
[28] Fayman YC. Microstructural characterization and elemental partitioning in a direct-aged superalloy (DA 718). Mater Sci Eng 1987;92:159–71.
[29] Burke MG, Miller MK. Precipitation in alloy 718: a combined Al3M and apfim investigation. In: *Superalloys 718, 625 and various derivatives*, warrendale, PA, USA, the minerals. Metals & Materials Society; 1991. p. 337–45.
[30] Devaux A, Naze L, Molins R, Pineau A, Organista A, Guedou JY, Uginet JF, Heritier P. Gamma double prime precipitation kinetic in alloy 718. Mater Sci Eng, A 2008;486:117–22.
[31] Liao YS, Lin HM, Wang JH. Behaviors of end milling inconel 718 superalloy by cemented carbide tools. J Mater Process Technol 2008;201(1–3):460–5.

[32] Tech Steel & Materials. Nickel inconel 718 AMS 5662. Tech Steel & Materials; 2022 [Online]. Available: https://www.techsteel.net/alloy/nickel/inconel-718/ams-5662. [Accessed 23 May 2022].
[33] Nicolay A, Franchet J-M, Bozzolo N, Cormier J. Metallurgical analysis of direct aging effect on tensile and creep properties in inconel 718 forgings. In: *Superalloys 2020*, warrendale, PA, USA, the minerals. Metals & Materials Society; 2020. p. 559–69.
[34] Haldipur P, Margetan FJ, Thompson RB. Estimation of single-crystal elastic constants from ultrasonic measurements on polycrystalline specimens. Review of Quantitative Nondestructive Evaluation 2004;23:1061–8.
[35] Rose JL. The christoffel equation for anisotropic media. In: Ultrasonic waves in solid media. Cambridge, UK: Cambridge University Press; 1999. p. 27–33.
[36] Azadian S, Wei L-Y, Warren R. Delta phase precipitation in Inconel 718. Materials Characterisation 2004;53:7–16.
[37] Chandler H. Heat Treater's guide: practices and procedures for nonferrous alloys. Materials Park, OH, USA: ASM International; 1996.